Method for Converter Synchronization with RF Injection

Joshua P. Bruckmeyer *jbruckme@harris.com*
Space and Intelligence Systems
Harris Corporation
Melbourne, FL- 32902, USA

Ivica Kostanic *kostanic@fit.edu*
Department of ECE
Florida Institute of Technology
Melbourne, FL- 32901, USA

Abstract

This paper presents an injection method for synchronizing analog to digital converters (ADC). This approach can eliminate the need for precision routed discrete synchronization signals of current technologies, such as JESD204. By eliminating the setup and hold time requirements at the conversion (or near conversion) clock rate, higher sample rate systems can be synchronized. Measured data from an existing multiple ADC conversion system was used to evaluate the method. Coherent beams were simulated to measure the effectiveness of the method. The results show near theoretical coherent processing gain.

Keywords: Time Dissemination, Sampled Data Circuits, Calibration, Array Signal Processing, and Phased Arrays.

1. INTRODUCTION

Radio Frequency (RF) sampling ADCs are replacing entire Intermediate Frequency (IF) sampling and Zero Intermediate Frequency (ZIF) sampling subsystems, lowering the overall system power [1]. As this technology matures, it is pushing converters to antenna enabling phased array antennas with elemental digital beam formers. The key is to ensure every converter adds coherently; this requires array level synchronization [2].

Modern converters support synchronization with a chip reset and/or auto sync function. For example the emerging JESD204B standard provides two mechanisms to support synchronization across several converters. Both methods require a synchronization signal to arrive at each converter in the system at the same time [3]. The key is to ensure that the setup and hold time of the synchronization signal relative to the clock is met across the entire span of data converters [3][4]. This is impractical at best at high sample rates (above a Gigahertz) and in distributed arrays.

The authors of [2] proposed a closed-loop deterministic phase synchronization algorithm as a solution to distributed synchronization. Their method estimates the phase offset from each transmitter and uses a feedback channel to command the transmitter to adjust its output phase in a multiple input single output (MISO) system [2]. By expanding this method to a multiple input multiple output (MIMO) or single input multiple output (SIMO) system, the receiver can perform the phase adjustment, eliminating the receiver to transmitter feedback network. Furthermore, if an internal injection calibration is used, the multiple output system can be synchronized without an external corporative transmitter.

In [5] the authors proposed adaptively equalizing the channel mismatches in time-interleaved ADCs (TIADCs) by injecting a known training signal into the ADC input. Since the analog input and clock signal split after ADC input, they become part of the calibration loop itself. The authors

showed that this method could mitigate interleaving spurs while avoiding complicated error estimation or measurement. To expand this method to synchronizing several ADCs inputs, a distribution network is needed for the training signal. Since this distribution network will not be used for normal operation, its characteristics need to be de-embedded.

Research on injection calibration for narrow band bean formers is also well established. The authors of [6] studied an injection method, where a transmitted output is switched into all of the receive channels. The goal stipulated is to correct amplitude and phase errors between the channels. By expanding this method to estimate and correct for temporal delays, the injection calibration method could correct for amplitude, phase, and temporal errors.

This paper expands upon the existing body of research by providing a converter synchronization method that is not subject to the setup and hold time limitations of discrete signaling. An RF injection method is proposed to correct time and phase delays between the converters. This proposed method addresses the physical implications of clock and data routing and is easily scaled to support several converters. A method to de-embed the contributions from the calibration network itself will also be presented.

2. METHODOLOGY

To establish a representative context basis, a system model is first described. The system serves as the basis for the mathematical assumptions and boundary conditions. The synchronization method and sub functions are then described.

2.1 System Model

The injection calibration system spans RF to digital signal processing (DSP) fabric as shown in figure 1. The DSP fabric contains a baseband calibration signal generator to generate a pseudorandom signal, d. This calibration signal is modulated onto an RF carrier and is represented by d'. The signal d' is injected into the RF analog input $\mathbf{x}$, forming $\mathbf{x}'$. Where $\mathbf{x}'$ is a P x 1 vector, where P is the number of phase centers (converter channels). The DSP fabric then uses training information, d, to synchronize the P phase centers in time.

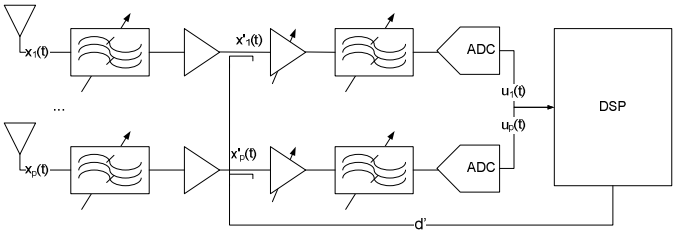

FIGURE 1: System Block Diagram.

2.2 Assumptions and Boundary Conditions

We start with the assumption that the input signal is observed by each of the phase centers. We also assume the presence of an additive white Gaussian noise channel. Furthermore we assume that the transmitted signal is a data sequence that is linearly modulated onto a carrier. Therefore, we can represent the input in its equivalent complex baseband form as [7]:

$$\mathbf{x}(t) = \mathbf{s}(t) + \mathbf{q}(t) \tag{1}$$

Where $\mathbf{s}(t)$ is a modulated signal, $\mathbf{q}(t)$ represents zero mean additive noise which is independent of the data [7], and all vectors are P x 1 in dimension. Assuming the training injection operation is an unbiased linear operation, $\mathbf{x}'$ can be represented in its baseband equivalent form as [8]:

$$\mathbf{x}'(t) = \mathbf{cf} \circ \left[\mathbf{s}(t) + \mathbf{q}(t)\right] \tag{2}$$

The vector $\mathbf{cf}(f)$ is the calibration factor that compensates the circuits outside the calibration loop and the inherent skew of the calibration network. The symbol $\circ$ is the Hadamard product matrix operator commonly referred to as the element multiplication. All vectors are P x 1 in dimension. The vector $\mathbf{cf}(f)$ can be directly measured with standard network analyzer equipment [9], or measured as a residual calibration vector on the system output after the calibration process has been completed [10][11].

The channel $\mathbf{u}$ output contains the coherently down-converted and digitized signal for all P phase centers. Assuming a well sampled signal and that ADC quantization noise has a negligible contribution, the channel output may be described as:

$$\mathbf{u}(t) = \left[\mathbf{x}'(t) + d'(t)\right] \circ \mathbf{h} \tag{3}$$

Assuming the following two factors: (1) a well-designed calibration signal, $d'(t)$, that does not correlate to input signal, $\mathbf{x}(t)$, and (2) that the ADC quantization noise has a negligible contribution , the input to the DSP can be expressed as:

$$\mathbf{u}(n) \cong d(n) \cdot \mathbf{h} \;\mid\; E\left[\mathbf{x}'(t) \cdot d'(t)\right] \cong 0 \tag{4}$$

This equation bounds the problem and variables for the synchronization process: where $\mathbf{u}(n)$ is estimated by direct measurement, $d(n)$ is a priori known to the system and $\mathbf{h}$ is the variable being solved for.

2.3 Synchronization Method

A representative synchronization circuit is shown in figure 2. The method is based on the well-known cross correlation technique to establish the course sample alignment between the channels [12].

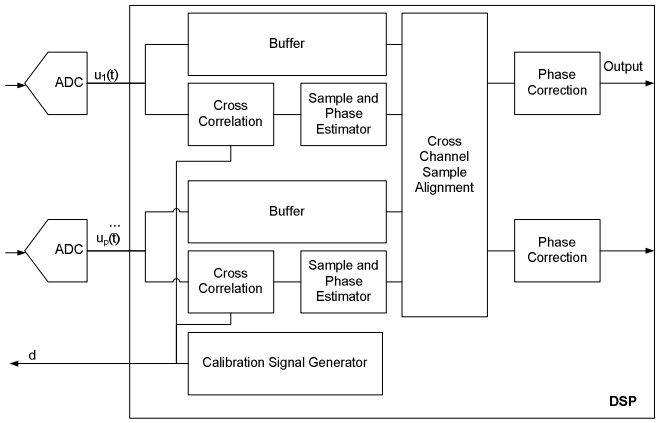

FIGURE 2: Synchronization Method.

For this synchronization method, the key technique is how to estimate the sample and sub-sample (phase) differences between the channels. To get the desired output, the following steps are proposed:

Step 1: The calibration signal generator authors a known baseband modulated signal. The calibration signal, d, is modulated outside the DSP fabric on an RF carrier and injected into the circuit. This injection can be as simple as an RF switch or, as shown, an RF coupler.

Step 2: The DSP fabric performs a cross correlation between the received signal, $\mathbf{u}$, and the known calibration signal, d, for all phase centers. The ADC samples are also buffered to account for the processing delay of the cross-correlation and phase estimator steps.

Step 3: The sample and sub-sample (phase) difference between the phase centers is estimated. The integer sample delay is the sample index that contains the peak cross-correlation energy [13]:

$$\mathbf{R}(\tau) = E[d(t) \cdot \mathbf{u}(t-\tau)] \tag{5}$$

$$\Delta\mathbf{t} = \arg_{\tau} \max[\mathbf{R}(\tau)] \tag{6}$$

The residual phase can be estimated by the complex angle of the peak cross-correlation energy [14]:

$$\theta = \arg_{\tau} \angle[\mathbf{R}(\tau)] \tag{7}$$

Step 4: Samples are read out of the buffer starting at the estimated $\Delta\mathbf{t}$ for each phase center. The depth of the buffer defines the amount of temporal channel-to-channel skew this method can compensate for.

Step 5: The conjugant of the phase estimated in Step 3 is applied to each phase center. This completes the temporal alignment of all of the phase centers to the calibration signal, d.

2.4 De-embedding Residual Offsets

To remove the temporal effects of the portion of the circuit not spanned by the calibration loop, an external calibration signal is required. The following steps can be used to de-embed these offsets:

Step 1: In any practical system there will be amplitude and phase differences between the external illumination signal and the phase centers. A calibrated external test apparatus, such as a network analyzer, should be used to measure this. Let $\mathbf{TS}$ be the P x 1 complex vector that has the channel-to-channel illumination differences.

Step 2: Use the synchronization method described in the synchronization method section to temporally align the internal calibration network.

Step 3: Estimate the residual channel-to-channel steering vector of the illumination waveform. There are many methods and waveforms available to do this. One common method is singular value decomposition using a continuous-wave (CW) signal. A convenience matrix, $\mathbf{Rxx}$, is formed by:

$$\mathbf{Rxx} = \sum_{n} \mathbf{u}(:,n) \cdot \mathbf{u}(:,n)' \tag{8}$$

Where the symbol, $:$, represents all P channels, and the symbol, $'$, is the complex transpose.

Eigenvalue decomposition is used to solve for the eigenvectors. The eigenvalue with the highest energy is assumed to correspond to the illumination waveform [15].

$$[\mathbf{V}, \mathbf{D}] = eig(\mathbf{Rxx}) \tag{9}$$

$$index = \arg_{n} \max \left| diag(\mathbf{D}) \right| \tag{10}$$

Finally, the steering vector representing the channel-to-channel estimate, $\mathbf{SV}$, is formed by normalizing the Eigenvector.

$$\mathbf{SV} = \frac{\mathbf{V}(:, index)}{\left\|\mathbf{V}(:, index)\right\|} \tag{11}$$

Step 4: Remove the test setup, $\mathbf{TS}$, bias:

$$\mathbf{CalVector} = \frac{\mathbf{SV}}{\mathbf{TS}^*} \tag{12}$$

The Calibration Vector, $\mathbf{CalVector}$, is a P x 1 complex vector containing the residual calibration vector, and the symbol, *, is the complex conjugant. Applying this vector can align all phase centers at an approximate zero phase channel-to-channel offset.

2.5 Figure of Merit

To illustrate the performance of the proposed method, coherent beams are formed. If all of the ADC channels are ideally time aligned, they should coherently add and result in a 10*log10(P) power signal-to-noise gain [16].

To establish a performance improvement for both the pre- and post- synchronization cases, the non-coherent video power is defined as:

$$VideoPower = \sum\sum \mathbf{u} \odot \mathbf{u}^* \tag{13}$$

The steering vector used for the pre- synchronization beam is:

$$\mathbf{PreSV} = \frac{ones(P,1)}{\sqrt{P}} \tag{14}$$

The pre-synchronization video power is estimated by:

$$\mathbf{PreBeam} = \mathbf{PreSV}.' \cdot \mathbf{u} \tag{15}$$

$$\mathrm{Pre}Power = \sum \mathbf{PreBeam} \cdot \mathbf{PreBeam}^* \tag{16}$$

Where $\mathbf{PreBeam}$ is a 1 x n vector, n is the number of samples, and the symbol, .' , is a non-conjugant transpose. Similarly the post-synchronization video power is estimated by:

$$\mathbf{PostBeam} = \mathbf{CalVector}.' \cdot \mathbf{u} \tag{17}$$

$$PostPower = \sum \mathbf{PostBeam} \cdot \mathbf{PostBeam}^* \tag{18}$$

3. RESULTS AND DISCUSSION

To illustrate the system performance benefit from this method, simulations were performed using measured hardware characteristics. The measured data are from an existing multiple ADC elemental digital beam former array with elemental sample storage, also known as pre-detection (PRE-D) capability. Specifically, two dual channel Texas Instruments ADC10D1000 devices operating at 480 MSPS were used. The signal was injected at 225 MHz into all four channels and the chip-to-chip synchronization methods were disabled.

The power of the pre-synchronized channel response with a Pulse Position Modulation (PPM)

illumination waveform is shown figure 3. Notably, there is a clear temporal delay between the ADC channels. The coherent beam also shows clear destructive interference.

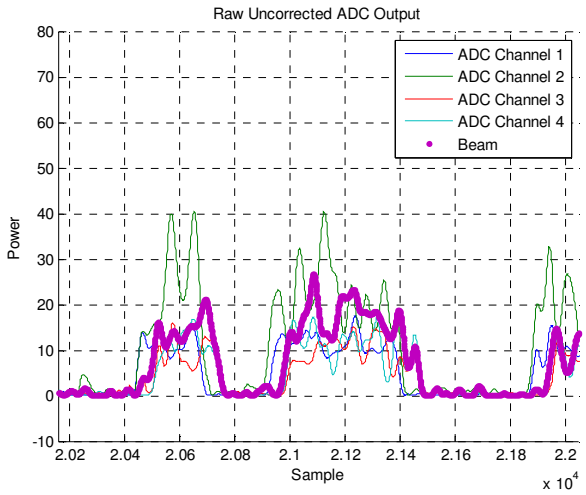

FIGURE 3: Pre-synchronization Signal.

In contrast the power of the post-synchronized channel response with the same PPM illumination waveform is shown in figure 4. All of the ADC channels are temporally aligned, and there is clear coherent beam gain.

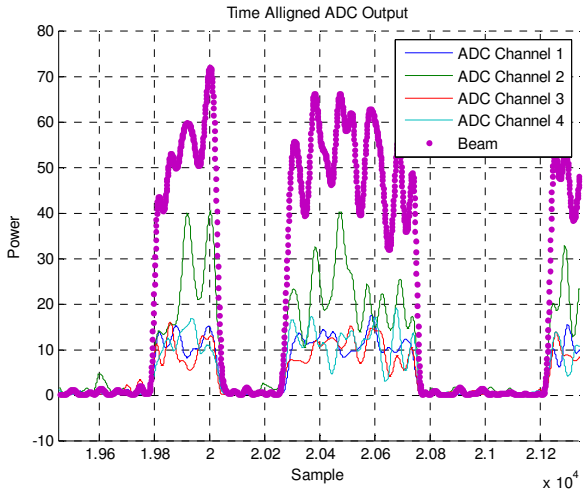

FIGURE 4: Post-synchronization Signal.

The numeric power estimates are shown in Table 1. As would be expected, the pre-synchronization beam shows a numeric loss in gain compared to the non-coherent video beam. In contrast, the post-synchronization method shows excellent performance, experiencing only 0.06 dB of loss compared to the optimal power combining of 6 dB.

Parameter	Raw Video	Pre-Sync. Beam	Post-Sync. Beam
Power (MW)	1.03	1.27	4.06
Gain from Raw (dB)	-	0.91	5.94

TABLE 1: Simulated Synchronization Gain.

The simulated performance is similar to the results from the Automatic Calibration method using Transmitting signals (ACT). The ACT method used an injected source to calibrate channel-to-

channel amplitude and phase errors with a single tap correction term. ACT resulted in 0.05 dB residual calibration error when calibrating a three phase center adaptive array [6]. The high degree of correlation in the results indicates the injection based synchronization method was successful in compensating for temporal delays without impacting system performance.

4. CONCLUSION AND FUTURE WORK

The simulation results show that injection based synchronization can be used to synchronize several data converts. The signal processing required is straight forward, and can readily be implemented in modern software defined radio fabric. Implementing this method can eliminate the need for discrete synchronization signals and lower the complexity of implementing distributed ADC systems.

Future work could focus on distribution of the injection signal over large distances to support distributed aperture systems. This could include the use of a distributed precision timing base, such as GPS, to synchronize the injection signal.

5. REFERENCES

[1] Texas Instruments Incorporated. “RF-Sampling and GSPS ADCs, Breakthrough ADCs Revolutionize Radio Architectures.” 2012, [On-line]. Available: www.ti.com/litv/pdf/snwt001 [Feb. 23, 2015].

[2] R. Hu et al. "A closed-loop deterministic phase synchronization algorithm for distributed beamforming." Wireless Communications and Networking Conference (WCNC), 2014 IEEE, pp.452,456, 6-9 April 2014.

[3] H. Saheb, S. Haider. "Scalable high speed serial interface for data converters: Using the JESD204B industry standard." Design & Test Symposium (IDT), 2014 9th International, vol., no., pp.6,11, 16-18 Dec. 2014.

[4] Texas Instruments Incorporated. “AN-2132 Synchronizing Multiple GSPS ADCs in a System: The AutoSync Feature.” 2013, [On-line]. Available: www.ti.com/lit/an/snaa073f/snaa073f.pdf [Feb. 27, 2015].

[5] S. Liu et al. "Adaptive Calibration of Channel Mismatches in Time-Interleaved ADCs Based on Equivalent Signal Recombination." Instrumentation and Measurement, IEEE Transactions on, vol.63, no.2, pp.277,286, Feb. 2014.

[6] K. Nishimori et al. "Automatic calibration method using transmitting signals of an adaptive array for TDD systems." in Vehicular Technology, IEEE Transactions on, vol.50, no.6, pp.1636-1640, Nov 2001

[7] M. Stojanovic, J.A. Catipovic, J.G. Proakis. "Reduced-complexity simultaneous beamforming and equalization for underwater acoustic communications." OCEANS '93. Engineering in Harmony with Ocean. Proceedings, pp.III426, III431 vol.3, 18-21 Oct 1993.

[8] S. Haykin. Adaptive Filter Theory, Upper Saddle River, New Jersey, Prentice Hall, 2002.

[9] K. R. Dandekar et al., "Smart antenna array calibration procedure including amplitude and phase mismatch and mutual coupling effects." Personal Wireless Communications, 2000 IEEE International Conference on, pp. 293-297, 2000.

[10] E. Lier et al. "Phased array calibration and characterization based on orthogonal coding: Theory and experimental validation." in In Phased Array Systems and Technology (ARRAY), 2010 IEEE International Symposium on, 2010.

[11] S. D. Silverstein. "Application of orthogonal codes to the calibration of active phased array antennas for communication satellites." Signal Processing, IEEE Transactions on 45, no. 1, pp. 206-218, 1997.

[12] B. Razavi. "Problem of timing mismatch in interleaved ADCs." in CICC, pp. 1-8. 2012.

[13] Y. Zhang and A. H. Waleed. "A comparative study of time-delay estimation techniques using microphone arrays." Department of Electrical and Computer Engineering, The University of Auckland, School of Engineering, 2005.

[14] S.L. Marple Jr. "Estimating group delay and phase delay via discrete-time “analytic” cross-correlation." Signal Processing, IEEE Transactions on , vol.47, no.9, pp.2604,2607, Sep 1999

[15] R. Adve. "Direction of Arrival," [On-line]. Available: http://www.comm.utoronto.ca/~rsadve/Notes/DOA.pdf [Sep. 4, 2015].

[16] I. Kostanic. "RF Propagation Lecture 12," [On-line]. Available: http://my.fit.edu/~kostanic/RF%20Propagation/New%20Notes/Lecture%2014.pdf [Dec. 27, 2014].